Supporting Information

A Comprehensive Study of Sulfonated Carbon Materials as Conductive Composites for Polymer Solar Cells

Ting Ji[1], Licheng Tan[1,2], Xiaotian Hu[1], Yanfeng Dai[1], Yiwang Chen[*1,2]

[1]College of Chemistry/Institute of Polymers, Nanchang University, 999 Xuefu Avenue, Nanchang 330031, China; [2]Jiangxi Provincial Key Laboratory of New Energy Chemistry, Nanchang University, 999 Xuefu Avenue, Nanchang 330031, China

Synthesis of sulfonated carbon nanotubes[1] and sulfonated graphene[2]

Pristine carbon nanotubes (P-CNTs) were first sonicated in the mixture of 1:1 concentrated HNO_3 (65%) and HCl (37%) for 1 h, these steps can remove catalyst particles around CNTs and also introduced oxygen-containing groups, mainly carboxyl groups on the CNTs. We defined them as F-CNTs in the following text. The F-CNTs were filtered and washed for times, then dried at 120 ºC in the vacuum overnight. Then 60 mg concentrated H_2SO_4 (98%) and 80 mg f-CNTs were mixed in a dry flask and then sonicated for 1 h, followed by heating to 260-300 ºC (The sulfuric acid boils at 335.5 ºC) with an electrical hand blender under nitrogen atmosphere for 20 h. After this treatment, the suspension was diluted by water and filtered. The production were washed to remove excess acid and frozen in a refrigerator, then dried in a freeze-drying chamber to obtain sulfonated CNTs (S-CNTs).

Synthesis of graphene oxide (GO) and reduced graphene oxide (RGO)

* Corresponding author. Tel.: +86 791 83969562; fax: +86 791 83969561. *E-mail address*: ywchen@ncu.edu.cn (Y. Chen).

The GO dispersion was prepared using Hummers-method as described previously. As a typical run, (1) 5.0 g of graphite power was added into a mixture of 5.0 g of $NaNO_3$ and 120 mL of H_2SO_4 (98%) in a 500 mL flask. (2) After stirring for 30min in an ice bath. (3) After stirring at room temperature over 12 h, the mixture gradually became paste-like and the color turned light brownish. (4) After the addition of 300 mL water under stirring, the mixture was heated to 98 ºC in a short time and kept at this temperature for 24 h, giving a yellow sample. (5) 100 mL of H_2O_2 (50wt%) was added to the mixture, stirring for 24 h at room temperature. (6) After rinsing and centrifugation with 5% HCl and deionized water several times, the GO dispersion was obtained. RGO was synthesized by the chemical reduction of GO using sodium borohydride. As a typical run, 0.5 g of the GO dispersion was added into water (500 mL), followed by sonication for 30 min. Then, 1.2 g of sodium borohydride was added into the mixture, heating at 100 ºC for 24 h. After repeated washing with water and centrifugation, and dispersing in the water, RGO was finally obtained.

Hydrothermal sulfonation of graphene (S-Gra)

S-graphene was synthesized from the hydrothermal sulfonation of S-graphene using fuming sulfuric acid at 180 ºC.As a typical run, 1.0 g of RGO was added into 50 mL of fuming sulfuric acid. After sonication for 30 min, the mixture was transferred into an autoclave to heat at 180 ºC for 24 h under stirring. After washing with a large amount of water and drying at 80 ºC for 12 h under vacuum, S-graphene was finally obtained.

Work function measurement

For the UPS measurements, He I (21.22 eV) radiation line from a discharge lamp was used, with an experimental resolution of 0.15 eV. All the UPS measurements of the onset of photoemission for determining the work function were done using standard procedures with a -5 V bias applied to the sample. The work function[3] was determined by the following equation, work function = hν-(E_{cutoff} - E_{onset}), where hν was incident photo energy (21.2 eV) of He Ⅰ , the high binding energy cutoff (E_{cutoff}) and HOMO region (E_{onset}) were the turing points. The E_{cutoff} was determined by linear extrapolation to zero at the yield of secondary electrons, and the E_{onset} was the onset relative to the Femi level (E_f) of Au (0 eV), where the E_f was determined from the Au substrate.

General measurements and characterizations

The Fourier transform infrared (FT-IR) spectra were recorded on a Shimadzu IRPrestige-21 Fourier transform infrared spectro-photometer by using KBr substrates. The X-ray diffraction (XRD) patterns of the composites were carried out on a Bruker D8 focus X-ray diffractometer operating at 30 kV and 20 mA with a copper target (λ =1.54 Å) and at a scanning rate of 1 °/min. Transmittance spectra were analyzed by UV-vis spectroscopy (Perkin Elmer Lambda 750). XPS studies were performed on a thermo-VG scientific ESCALAB 250 photoelectron spectrometer using a monochromated AlKa (1,486.6 eV) X-ray source. All recorded peaks were corrected

for electrostatic effects by setting the C-C component of C 1s peak to 284.8 eV. Sheet resistances of electrodes were measured by using a four point probe. Contact angle measurements for all samples were characterized on a contact angle instrument (JC2000A) with deionized water obtained from ultrapure water system and hexadecane purchased from Shanghai TCI chemical (98%, AR). For the ultraviolet photoelectron spectroscopy (UPS) measurements, He I (21.22 eV) radiation line from a discharge lamp was used with an experimental resolution of 0.15 eV. The onset of photoemission for determining the work function was calculated using standard procedures with a -5 V bias applied to the sample. The work function was determined by the UPS (see Supporting Information). The morphologies of composites were investigated by scanning electron microscopy (SEM) using a QuanTA-200F. Atomic force microscopic (AFM) images were measured on a nanoscope III A (Digital Instruments) scanning probe microscope using the tapping mode. Transmission scanning electron microscopy (TEM) images were recorded using a JEOL-2100F transmission electron microscope and an internal charge-coupled device (CCD) camera. The thicknesses of all films were measured by surface profilometer (Ambios Technology Ltd. XP-2).

Space-charge-limited-current (SCLC) mobility measurement

In order to characterize the carrier mobility of modified device, the hole-only devices were fabricated. The hole-only devices was built as ITO/PEDOT:PSS/P3HT:PCBM/MoO_3/Ag. The carrier mobility was measured using

the SCLC model at low voltage[4] which is described by (Equation 1):

$$J=9\varepsilon_0\varepsilon_r\mu V^2/8L^3 \quad (1)$$

Where ε_0 is the permittivity of free space (8.85×10^{-12} F m^{-1}), ε_r is the dielectric constant of P3HT or PCBM (assumed to 3), μ is the mobility of an electron, V is the applied voltage, and L is the film thickness[4,5]. The thickness of the BHJ blend for SCLC measurement was about 120 nm. By fitting the results to a space-charge-limited form, $J^{0.5}$ versus V is plotted in **Figure 1**.

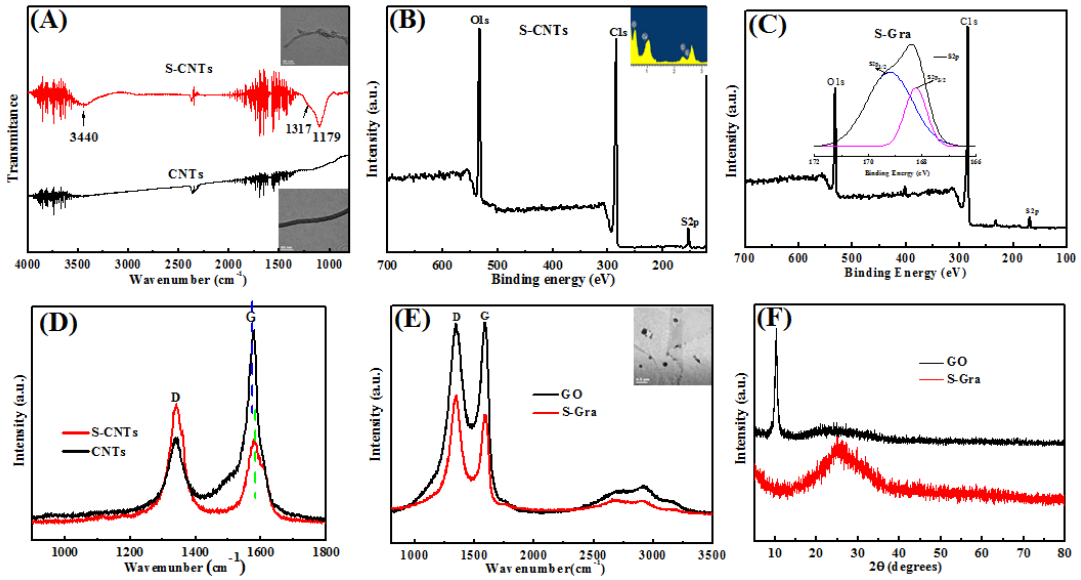

Figure S1. (A) FTIR spectra of pristine CNTs and S-CNTs, (B) XPS survey spectrum of S-CNTs, (C) XPS survey spectrum of S-Gra, (D) Raman spectra of S-CNTs and pristine CNTs, (E) Raman spectra of GO and S-Gra, and (F) XRD profiles of GO and S-Gra. The insets in figure A are the TEM images of S-CNTs and pristine CNTs. The insets in figure B, C E show the EDS analysis of S-CNTs, S2p peak of S-Gra and TEM image of S-Gra.

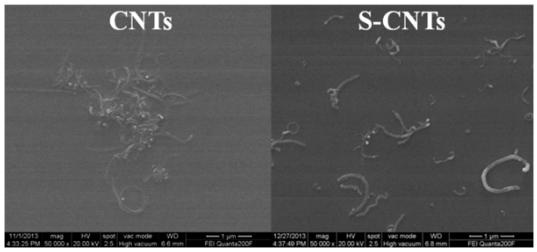

Figure S2. SEM images of pristine CNTs and S-CNTs in DMSO solvent (1 mg/mL).

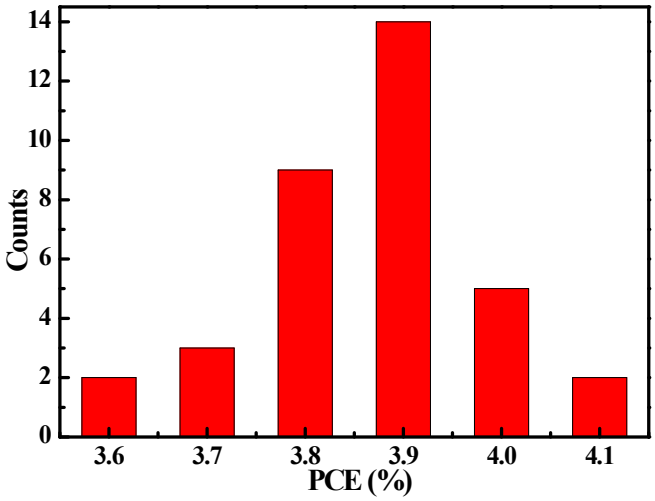

Figure S3. Histogram of solar cell efficiencies for 35 devices: ITO/PEDOT:PSS:S-CNTs (0.2%)/P3HT:PCBM/LiF/Al.

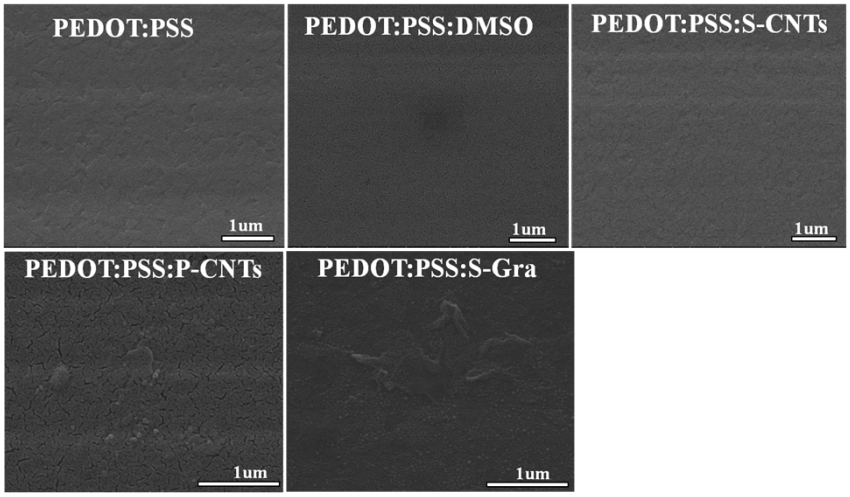

Figure S4. SEM images of the pristine and modified PEDOT:PSS. P-CNTs, S-CNTs and S-Gra were added into PEDOT:PSS at 0.2% weight ratio. To make a comparison, PEDOT:PSS was treated with DMSO at same ratio.

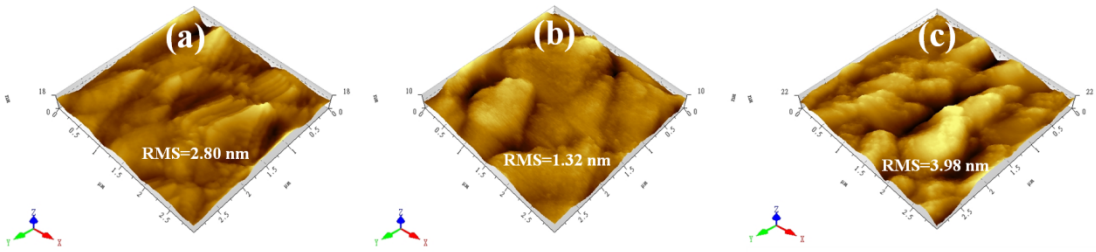

Figure S5. Tapping-mode atomic force microscopy (AFM) three-dimensional (3 × 3 um) images of (a) PEDOT:PSS/P3HT:PCBM, (b) PEDOT:PSS:S-CNTs (0.2%)/P3HT:PCBM and (c) PEDOT:PSS:S-Gra (0.2%)/P3HT:PCBM.

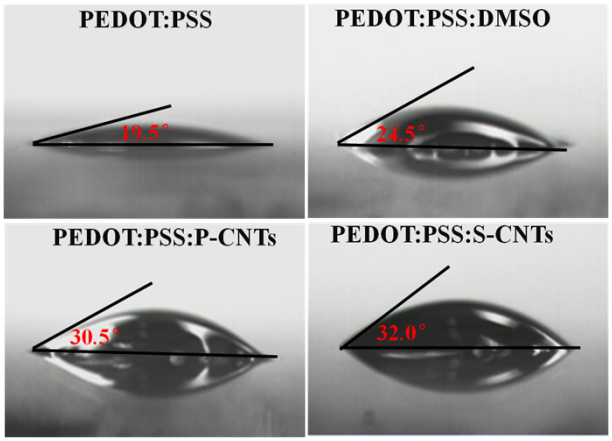

Figure S6. Contact angle measurements of the pristine and modified PEDOT:PSS. P-CNTs, S-CNTs and S-Gra were added into PEDOT:PSS at 0.2% weight ratio. To make a comparison, PEDOT:PSS was treated with DMSO at same ratio.

The interaction between S-CNTs and PEDOT:PSS would also affect the hydrophilicity-hydrophobicity of the modified PEDOT:PSS, so the contact angle was further investigated, as shown in **Figure S6**. The PEDOT:PSS treated with P-CNTs, S-CNTs show contact angles of 26.5º, 34.0º, respectively, which are bigger than that of pristine PEDOT:PSS. Moreover, the contact angle of PEDOT:PSS:P-CNTs is similar to that of PEDOT:PSS:DMSO (27.0º), which indicates that the alteration of contact angle for PEDOT:PSS:P-CNTs is ascribed from the DMSO solvent effect, instead of the addition of pristine CNTs. The increased contact angle of the PEDOT:PSS:S-CNTs is related to the depletion of hydrophilic PSS chains attributed to the synergetic effect between S-CNTs and PEDOT:PSS, and consequently increasing hydrophobic PEDOT grains on the surface of the film. The optimized hydrophobicity of PEDOT:PSS:S-CNTs could result in better interface contact between the modified PEDOT:PSS and active layer, which would boost the device performance.

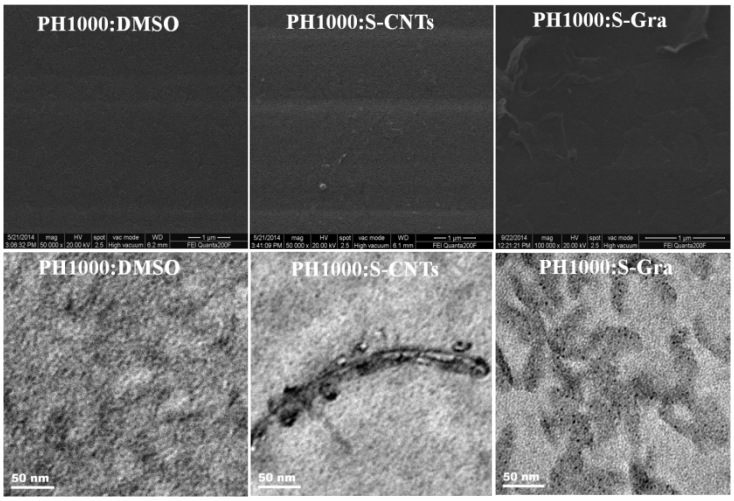

Figure S7. SEM and TEM images of modified PH1000. S-CNTs and S-Gra were added into PEDOT:PSS at 1.0% weight ratio. To make a comparison, PEDOT:PSS was treated with DMSO at same ratio.

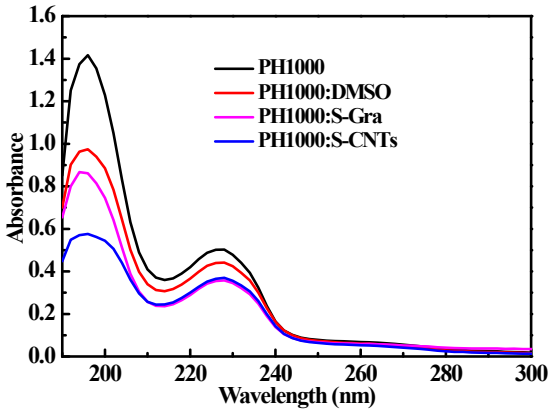

Figure S8. UV absorption spectra of the pristine and modified PH1000. S-CNTs and S-Gra were added into PEDOT:PSS at 1.0% weight ratio. To make a comparison, PEDOT:PSS was treated with DMSO at same ratio.

Table S1. Superficial PSS/PEDOT ratios of the pristine and modified PEDOT:PSS.

	PEDOT:PSS	DMSO	P-CNTs (0.2%)	S-CNTs (0.2%)
PSS/PEDOT	11.0	8.7	8.6	7.5

Table S2. The electrical and optical properties of modified PH1000 electrodes.

	R_{sheet}	Transmittance (%, at 550 nm)	$\sigma_{DC}/\sigma_{Op}(\lambda)$
PH1000	140.5	85.3	16.3
PH1000:DMSO	125.7	84.4	16.78
PH1000:S-CNTs	81.8	85.3	27.6
PH1000:S-Gra	45	85.5	51.6

References

(1) H. Yu, Y. Jin, Z. Li, F. Peng, H. Wang, *J. Solid State Chem.*, 2008, ***181***, 432-438.

(2) F. Liu, J. Sun, L. Zhu, X. Meng, C. Qi, F.-S. Xiao, *J. Mater. Chem.*, 2012, ***22***,5495-5502.

(3) J. H. Seo, A. Gutacker, Y. Sun, H. Wu, F. Huang, Y. Cao, U. Scherf, A. J. Heeger, G. C. Bazan, *J.Am. Chem. Soc.*, 2011, ***133***, 8416-8419.

(4) Y. Liu, X. Wan, F. Wang, J. Zhou, G. Long, J. Tian, Y. Chen, *Adv. Mater.*, 2011, ***23***,
5387-5391.

(5) Y.-J. Cheng, C.-H. Hsieh, P.-J. Li, C.-S. Hsu, *Adv. Funct. Mater.*, 2011, ***21***, 1723-1732.